Supplemental Information Neuron, Volume 67

Differences in Gamma Frequencies across Visual Cortex Restrict Their Possible Use in Computation

Supratim Ray and John H.R. Maunsell

Inventory of Supplemental Material

Supplementary Figure 1: Explains the Experimental Tasks performed by the monkeys.

Supplementary Figure 2: Shows the effect of attention on firing rates and gamma oscillation frequencies (related to Figure 1).

Supplementary Figure 3: Shows the spike-spike coherence as a function of stimulus contrast (related to Figure 2 which shows the LFP-LFP and spike-LFP coherence). This supplementary figure also shows the results of some simulations to compare the sensitivity of different measures of spike-LFP versus spike-spike synchronization.

Supplementary Figure 4: Shows the spike-spike coherence as a function of electrode distance (related to Figure 5 which shows the LFP-LFP and spike-LFP coherence).

Supplementary Figure 1

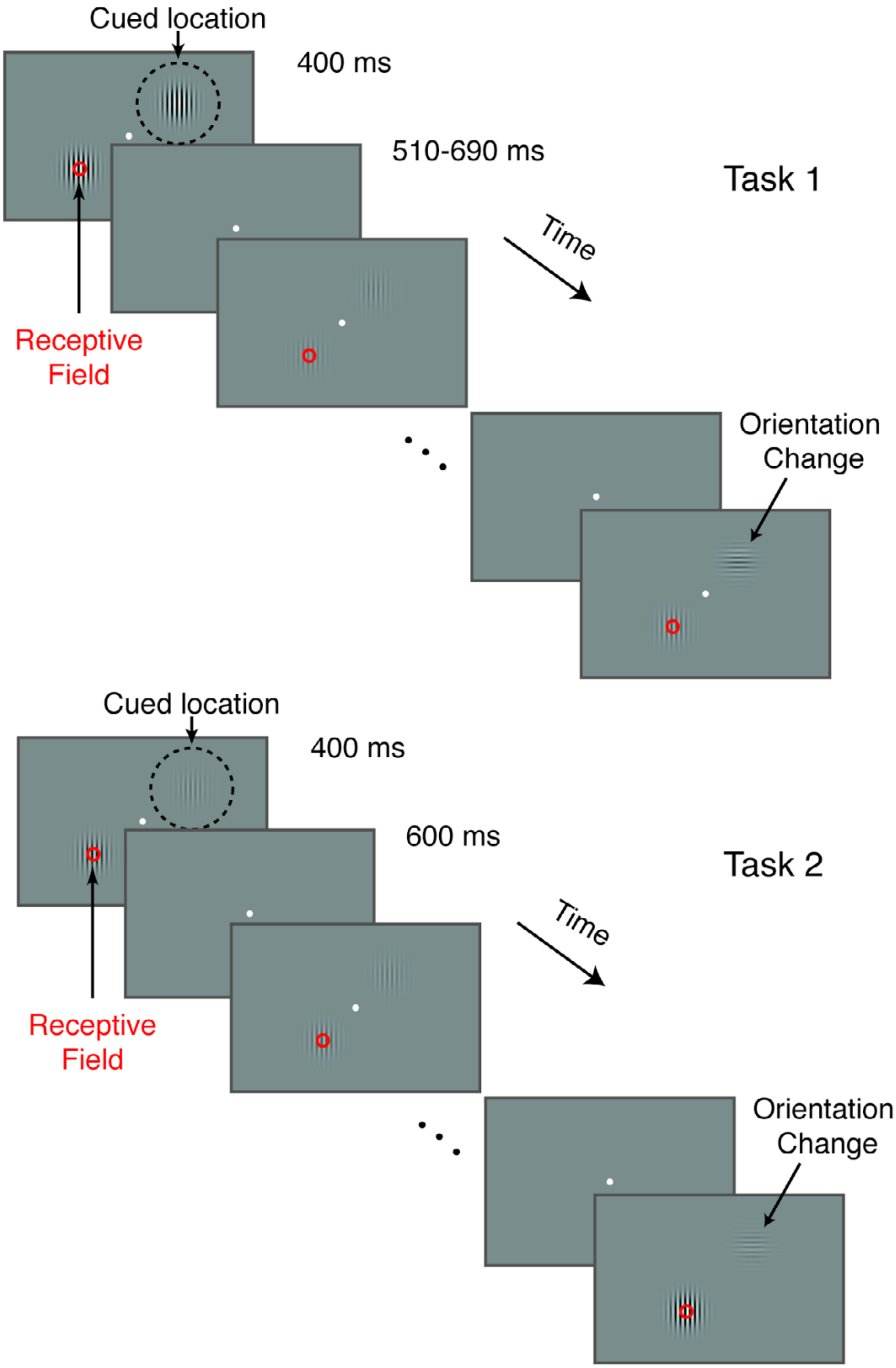

Supplementary Figure 1: *Task Design*. Monkeys were trained to do two versions of an orientation-change detection task, Task 1 (upper plot; an attention experiment for which the contrasts of the stimuli inside and outside the receptive field were matched) and Task 2 (lower plot; mainly used for studying the response properties of the neurons in the receptive field while maintaining the monkey's attention away from the receptive field). Task 1 was performed only by Monkey 1 and used only for the contrast study (Figures 1 and 2).

Supplementary Figure 2

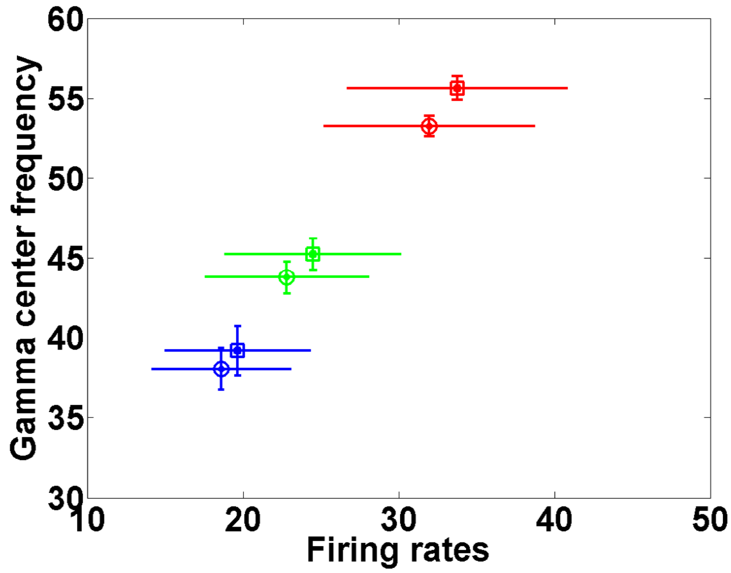

Supplementary Figure 2: *Effect of attention on firing rates and gamma frequency.* Mean firing rates and gamma center frequencies of the 28 electrodes for which >20 spikes were recorded and the SNR of the isolation was greater than 1.5 (same criteria used throughout the paper) for Monkey 1. Error bars are SEM. The circles are for the attend-out condition while the squares are for the attend-in condition. The three colors represent different contrasts (blue – 25%, green – 50%, red – 100%). The points fall on a line, suggesting that variations in firing rate would result in a fixed change in the gamma oscillation frequency, irrespective of whether that change in firing rate is caused by a change in stimulus contrast or a shift in attention.

Supplementary Figure 3

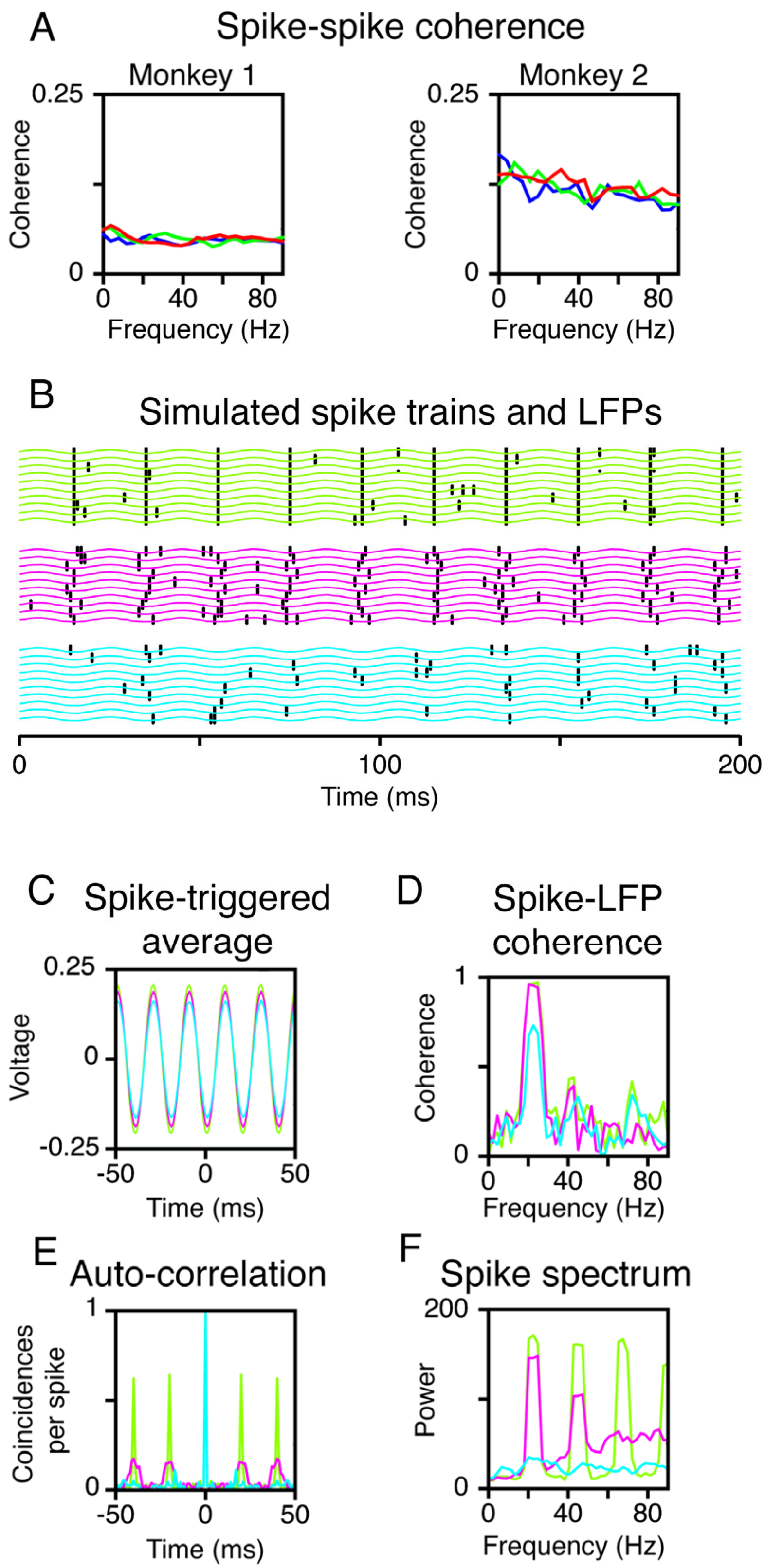

Supplementary Figure 3: *Comparison of different measures of synchronization.* A) Mean spike-spike coherence measured 150-406 ms after stimulus onset for 44 and 23 pairs of electrodes that 1) provided as least 20 spikes, 2) had receptive field centers within 0.2 degrees of the stimulus center, and 3) had a signal-to-noise ratio greater than 1.5. Different colors correspond to the different stimulus contrasts (blue - 25%, green – 50%, red – 100%). B) Simulated spike raster plot and LFP data to study the effect of spike jitter and spike firing probability on different measures of synchronization. Three conditions were simulated (shown in different colors, 10 traces for each condition). In each case, the LFP was simulated as a sinusoidal oscillation at 50 Hz (gamma rhythm). Green traces (top): Spikes were generated at the trough of each gamma cycle, with no jitter. In addition, to account for the baseline firing, we simulated a Poisson distributed spike train with mean of 10 spikes/s, which was the baseline firing rate in our dataset. The overall firing rate in this case was 60 spikes/s (50 spikes/s locked to the trough of the gamma cycle and 10 spikes/s randomly distributed with respect to the gamma cycle). Magenta traces (middle): Same as the condition above, but now spikes had a jitter of ± 2 ms, which was the average jitter observed in our dataset.. Blue traces (bottom): The spikes were generated at the trough of each gamma cycle with a probability of 0.3, and had a jitter of up to 2 ms. The firing rate was 25 spikes/s, which was the value observed in our dataset during the analysis period. C) Spike-triggered average of the simulated dataset. D) Spike-LFP coherence of the simulated dataset, computed using the multitaper method. E) Auto-correlation function of the spike trains (1 ms bin-width). F) Spike spectrum of the spike trains, computed using the multitaper method. With no jitter (green traces), all four measures showed significant peaks. With up to 2 ms jitter (magenta traces), however, the spike auto-correlation (E) and spike spectrum peaks (F) were reduced even though the spike-triggered average (C) and spike-field coherence were not (D). This is because each cycle of the gamma rhythm is 20 ms – a jitter of 2 ms still results in spikes approximately at the trough of the gamma cycle. However, spike-spike synchronization is measured at the resolution of 1 ms, for which a 2 ms jitter is substantial. Finally, changing the firing probability from 1 to 0.3 (magenta versus blue traces) resulted in only a modest decrease in the spike-triggered average and spike-field coherence, but the spike auto-correlation and spike spectrum peaks disappeared. This happens because spike spectrum and autocorrelation critically depend on the periodicity of the spikes. Spike-LFP measures, on the other hand, depend only on the relative position of the spike in the gamma cycle, and are much less sensitive to the absence of spikes in some gamma cycles.

Supplementary Figure 4

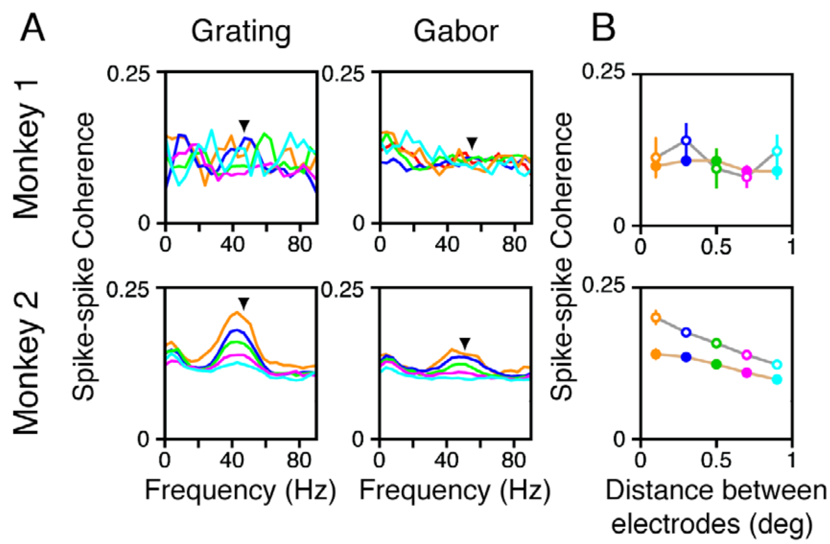

Supplementary Figure 4. *Spike-spike synchronization for the distance study* A) Spike-spike coherence for the grating (left column) and Gabor stimulus (right column), for Monkey 1 (upper row) and Monkey 2 (lower row). Same format as Figure 5. The data were averaged over 28 and 133 electrode pairs for the grating and Gabor stimuli for Monkey 1, and 1371 and 1609 pairs for Monkey 2. The spike-spike coherence values were smaller than the spike-LFP coherence values (shown in Figure 5) for all conditions. For Monkey 1, we did not observe any significant spike-spike synchronization, which could be due to the weaker sensitivity of spike-spike measures (as described in Supplementary Figure 3) as well as an insufficient number of electrode pairs. For Monkey 2, however, we observed significant spike-spike coherence, which was much stronger for the grating than for the Gabor and decreased monotonically with electrode distance (note that for this monkey we had a large number of electrode pairs, which increased the statistical power). B) The mean coherence values computed at the best gamma frequency (black inverted triangles in A, for different electrode distances. Open and filled circles (joined by gray and brown lines) represent the coherence values for the grating and Gabor stimuli. For Monkey 2, the two-way ANOVA yielded p-values of less than 10^{-16} for both stimulus and distance factors, and 0.03 for the interaction term. The results were similar after matching the electrode pairs for the two stimuli (952 electrode pairs). Note that the slight decrease in the difference between coherence values at higher electrode distances is merely a 'baseline effect' – at an electrode distance of 0.7 and 0.9 degrees the coherence spectra were almost flat for the Gabor stimulus (magenta and light blue traces in the lower right plot in A), so the coherence values showed a plateau at ~0.1, while the coherence values kept decreasing with distance for the grating. Overall, these data support the results from the spike-field coherence measures (Figure 5) that the synchronization in the network falls when a grating is replaced by a Gabor stimulus.